

Identifying the tilt angle and correcting the orbital angular momentum spectrum dispersion of misaligned light beam

Peng Zhao, Shikang Li, Yu Wang, Xue Feng*, Kaiyu Cui, Fang Liu, Wei Zhang, and Yidong Huang

Department of Electronic Engineering, Tsinghua National Laboratory for Information Science and Technology, Tsinghua University, Beijing, China

x-feng@tsinghua.edu.cn

Abstract

The axis tilt of light beam in optical system would introduce the dispersion of orbital angular momentum (OAM) spectrum. To deal with it, a two-step method is proposed and demonstrated. First, the tilt angle of optical axis is identified with a deduced relation between the tilt angle and the variation of OAM topological charges with different reference axes, which is obtained with the help of a charge coupled device (CCD) camera. In our experiments, the precision of measured tilt angle is about $10^{-4}rad$ with OAM orders of -3~3. Using the measured angle value, the additional phase delay due to axis tilt can be calculated so that the dispersion of OAM spectrum can be corrected with a simple formula while the optical axis is not aligned. The experimental results indicate that the original OAM spectrum has been successfully extracted for not only the pure OAM state but also the superposed OAM states.

Introduction

Since OAM was characterized as a new freedom of lightwave by Allen, et.al in 1992¹, it has been attracted much research interest and shown its potential on various applications. Due to the torque force^{2,3} and less radiation pressure deriving from the dark phase singularity⁴⁻⁶, light beam carrying OAM can serve as optical tweezers and spanners. Meanwhile, as the OAM states can form an infinite dimensional Hilbert space, it can be applied on encoding information for classical optical communications^{7,8} or high dimensional quantum entanglement^{9,10}.

As shown by Allen, *et.al*¹, under paraxial approximation, the angular momentum of light beam can be divided into two independent parts, spin angular momentum (SAM) and OAM. The SAM originates from the

polarization while the OAM is from the helical wavefront. Usually, Laguerre-Gaussian (LG) mode is utilized to investigate the properties of optical OAM since it is the eigenmode of paraxial wave equation in cylindrical coordinate and any paraxial beam can be decomposed as a series of LG modes. For LG mode with helical phase front of $\exp(-il\phi)$, in which ϕ is the azimuthal angle and l is azimuthal index, the OAM in the propagation direction has the discrete value of $l\hbar$ per photon. For such LG mode with nonzero l , the intensity distribution is a hollow ring with rotational symmetry by considering light propagation center as pivot. Thus, it is natural to treat this symmetry center as the axis of light beam and define the OAM along such axis. However, for real applications, there may be misalignment between axis of light beam and that of optical system so that the pure OAM state of an individual photon in a LG mode would transform to the superposition of some OAM states, which is known as the dispersion of OAM spectrum^{11,12}. Such misalignment can be introduced by the lateral displacement and (or) the tilt between the axes of light beam carrying OAM and optical system. Till now, there are some reports that have investigated such phenomena¹¹⁻¹⁵ and two methods that have been proposed to deal with it. In Ref. 14, Yi-Dong Liu, et.al have introduced the mean square value of OAM spectrum to quantize the degree of the lateral displacement and the tilt. Their numerical simulation results have shown that the mean square value monotonously increases following the rise of misalignment so that a feedback system was proposed to correct the misalignment step by step after measuring the mean square value of OAM spectrum. In Ref. 15, J. Lin, *et.al* have deduced the relationship of the dispersed OAM spectrum versus the tilt angle and lateral displacement. Based on such analytical formulation, the misalignment can be extracted from the OAM spectrum, which was proposed to be obtained from several coefficients one by one with the help of an optical correlator. Although both the lateral displacement and the tilt of the optical axis would introduce OAM spectrum dispersion, the latter is much more critical. This work is focused on this issue and a two-step method is proposed and demonstrated to identify the tilt angle and correct the dispersion of OAM spectrum. First the tilt angle is obtained from the variation of topological charge due to varied reference axes and then the OAM spectrum is corrected according to the tilt angle with a deduced simple formula. Compared with the previously proposed methods, our presented method is relatively simple since there is no additional feedback system¹⁴ or optical correlator¹⁵ required. Actually, only a CCD is required to obtain the Stokes parameter of S_0 and the phase distribution of incident light beam. Moreover, the original OAM spectrum of not only a pure OAM state but also a superposition of several OAM states can be well extracted according to our experimental results. At last, since both calculating the tilt angle and correcting the OAM spectrum are based on analytical formulae, these procedures can be automatically and fast done with a computer while there is no iteration required.

Result Section

Principle

Under the paraxial approximation, the eigenmode of paraxial wave equation in cylindrical coordinate (r, ϕ, z) is LG mode:

$$LG_p^l = \frac{a_{p,l}}{w} \left(\frac{\sqrt{2}r}{w} \right)^{|l|} L_p^{|l|} \left(\frac{2r^2}{w^2} \right) e^{-r^2/w^2} e^{ikr^2/2R} e^{il\phi}, \quad (1)$$

where $a_{p,l}$ is the normalizing coefficient, w is the width of the light spot, k is the wave vector, R is the curvature radius of the wavefront while p and l denote the radial and azimuthal mode index, respectively. l is also known as the topological charge of the carried OAM since each LG mode of LG_p^l carries OAM of $l\hbar$ and linear momentum of $\hbar k$ per photon along the propagation direction. Theoretically, the electric field of an arbitrary scalar light beam can be expressed as the superposition of LG modes.

$$E(r, \phi, z) = \sum_l \sum_p m_{lp} LG_p^l, \quad (2)$$

where m_{lp} denotes the weight factor of mode LG_p^l and the superposition among the azimuthal index would introduce the OAM spectrum:

$$C_l = \frac{\sum_p |m_{lp}|^2}{\sum_l \sum_p |m_{lp}|^2}. \quad (3)$$

The coefficient of C_l represents the power proportion of l -order OAM component over the total power. OAM spectrum plays an important role in many applications, especially in quantum information⁹, classic communication¹⁶ and optical imaging¹⁷. However, it is not easy to measure the OAM spectrum since it relies on the reference axis. In other words, misalignment in optical systems would lead to significant distortion on the spectrum.

For explaining it with more details, the simplest case, which is a free-space optical system only containing an OAM source and detector, is considered as a concrete example. According to Ref. [12] and [13], if there is the tilt or (and) the lateral displacement between the optical axis of the detector and source, the measured spectrum would deviate from the original spectrum emitted from OAM source. Even for a pure and single OAM state

emitted from the source, the measured spectrum would be broadened from a single peak to multiple lines on the OAM spectrum. To identify such phenomena, the dispersion of the OAM spectrum was defined as
$$v = \frac{\sum_l C_l l^2}{\sum_l C_l l} - \left(\frac{\sum_l C_l l}{\sum_l C_l} \right)^2$$
 in Ref. [12] and [13]. To avoid such dispersion, precise alignment is required while measuring the OAM spectrum. Actually, the axis tilt is much more sensitive than the position displacement to the variation on OAM spectrum. For example, the dispersion value would be about $v=1$ when the position displacement is about the size of light spot (typically several mm) or the tilt angle is about $2.5 \times 10^{-4} \text{ rad}$. Additionally, for state of the art technology, it is easy to correct the position displacement with accuracy of tens of nm, which is much smaller than the typical size of a light spot. But it is still a tough work to correct the tilt angle with accuracy of $\sim 10^{-4} \text{ rad}$. Thus, this work focuses on how to determine the tilt angle and correct the corresponding deviation on OAM spectrum.

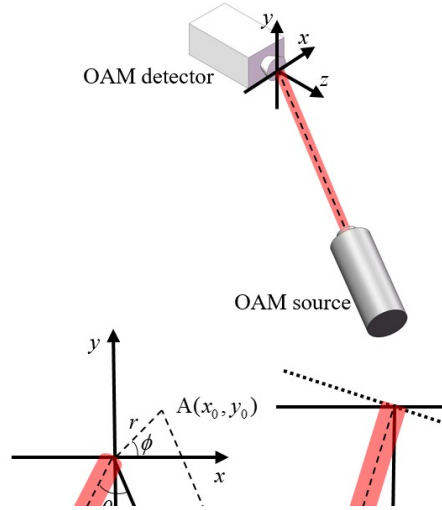


Fig. 1. Schematic figure of axis tilt between the OAM source and detector.

With the simplest example of only an OAM source and detector, the OAM detector is settled with the optical axis along the z -axis while there is a small tilt angle of incident OAM light beam. Without loss of generality, it is assumed that the optical axis of incident light beam is within the plane of the z -axis and minus x -axis while the small tilt angle of θ is defined by z -axis [Fig. 1]. After considering the axis tilt, the value of carried topological charge would depend on reference axis. To demonstrate it, another reference axis would be introduced as shown as the dashed line in Fig. 1, which is parallel to z -axis and the intersection point with the x - y plane is the point $A(x_0, y_0)$ named as z' -axis. It should be mentioned that here the Cartesian coordinate (x, y) is used for simplicity and clarity of demonstration. In latter simulations and experiments, cylindrical coordinate (r, ϕ) is adopted for convenience, and the relation between them relies on:

$$\begin{cases} x = r \cos \phi \\ y = r \sin \phi \end{cases} \quad (4)$$

l_z and l'_z denote the topological charge defined by the reference axis as z -axis and z' -axis, respectively. According to Ref. ¹³, the relation between l_z and l'_z is:

$$l'_z = l_z + \frac{-x_0 P_y + y_0 P_x}{\hbar}, \quad (5)$$

Where P_x and P_y denotes the x component and y component of transversal linear momentum of incident light beam, respectively. For the considered case, the axis tilt is within x - z plane for the sake of simplicity and the angle θ is small enough so that small-angle approximation of $\sin \theta \approx \theta$ can be adopted. Hence, the values of linear momentum are $P_x = \hbar k$ per photon and $P_y = 0$. Thus the variation between l_z and l'_z can be deduced from Eq. (5) as:

$$\Delta l = l'_z - l_z = y_0 k \theta \Rightarrow \theta = \frac{\Delta l}{y_0 k}. \quad (6)$$

From Eq. (6), it can be found that the variation of topological charge (Δl) is proportional to the tilt angle (θ). Thus, a simple method to measure small angle θ between light beam and the optical axis of detector can be obtained by measuring topological charge with different reference axis. Theoretically, only two different reference axes are required to measure Δl . However, to reduce the fluctuations in practical measuring process, multiple different reference axes can be adopted and the number is 21×21 in our experiments as shown in the Results section. Then the tilt angle can be obtained by linear fitting the measured topological charges with different reference axes.

After the tilt angle of θ is known, the most direct method to correct it is precisely adjusting the optical system. For some applications, such precise alignment is inevitable. For example, for optical wireless communication with OAM multiplexing ¹⁶, the optical axis of transmitter and receiver has to be aligned to avoid channel cross talk since different OAM mode serves as different transmission channel. However, for some applications where only the origin OAM spectrum is required, another option is to extract the measured OAM spectrum with the known tilt angle of θ . In the next section, a two-step method to measure θ and correct the measured OAM spectrum will be demonstrated based on our previous work ¹⁸.

The first step is to obtain the tilt angle of θ . The topological charges with different reference axis should be measured according to Eq. (6). In our previous work ¹⁸, the topological charge of arbitrary vectorial light beam can be expressed with Stokes parameters and Pancharatnam phase. For uniform polarized light beam considered here, the formula can be reduced as:

$$l = \frac{\iint -S_0 \frac{\partial \varphi}{\partial \phi} r dr d\phi}{\iint S_0 r dr d\phi}, \quad (7)$$

where S_0 , l , and φ denote Stokes parameters, the total topological charge, and the phase distribution of light beam, respectively, while r and ϕ denote the radial and azimuthal coordinates of cylindrical coordinate system, respectively, sharing the same origin and z -axis with the Cartesian coordinate system as shown in Fig. 1. Stokes parameters and the phase distribution can be obtained by measuring the intensities of light beam and the interference of light beam with one reference light, respectively.

The second step is extracting the measured spectrum. With Stokes parameters and the phase distribution, the OAM spectrum of light can be deduced as ¹⁹:

$$C_l = \frac{\iint S_0 e^{-il\varphi} e^{-il\phi} d\phi r dr}{\iint S_0 r dr d\phi}. \quad (8)$$

Under small axis tilt, the Stokes parameters could be treated a constant value while the variation of the phase distribution in x - y plane depends on the position. After considering the tilt angle, the phase distribution of light in the cross section would experience additional phase delay of $\Delta\varphi(x, y) = k\theta x$, as shown in Fig. 1. Thus, the measured phase distribution of φ_m should be corrected as $\varphi = \varphi_m + \Delta\varphi$ so that the original OAM spectrum can be obtained.

Experimental setup:

To verify our proposed method of measuring the tilt angle and correcting the dispersion of the OAM spectrum, a series of experiments have been carried out.

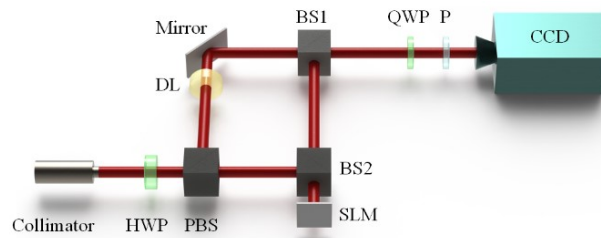


Fig. 2. The schematic of experimental arrangements. HWP: half-wave plate, PBS: polarizing beam splitter, BS: beam splitter, SLM: spatial light modulator, DL: delay line, QWP: quarter-wave plate, P: polarizer.

Figure 2 shows the schematic of experimental setup, which is a typical Mach-Zender interferometer arrangement. A laser operating at wavelength of 1550nm (RIO Orion) is connected with a collimator by a pigtail fiber so that the diameter of light beam is expanded to several millimeters and injected into the optical system. Followed the collimator, there are a half-wave plate (HWP) and a polarizing beam splitter cube (PBS) to split light beam into two orthogonal polarization components with controlled ratio. The horizontal polarization component is incident towards a beam splitter of BS2 and reflected to the spatial light modulator (SLM, PLUTO-TELCO-013). Then a pre-settled OAM mode would be generated through the SLM by modulating the phase of incident light, which is treated as the objective light. The vertical polarization component reflected by PBS would serve as the reference light for interference. Then the objective and the reference light beams would be combined by BS1 and a delay line (DL) is inserted within the optical path of reference light to control the phase delay. After BS2, the interference pattern would be detected by a CCD, in front of which there are a quarter-wave plate (QWP) and a polarizer (P) to filter out the right-hand circularly polarized component. The detected intensity pattern would be recorded and processed by a computer connected to the CCD.

As mentioned, Stokes parameter of S_0 and the phase distribution of objective light should be measured. The Stokes parameter of S_0 is related to the intensity of objective light, which can be directly obtained from CCD camera. To measure the phase distribution of objective light, we have measured the interference pattern between the objective and reference light. As shown in Fig.2, the objective light is OAM beam while the reference light is 0-order LG mode. Here, we denote the intensity and phase distribution of objective/reference beams on the plane of CCD camera as I_{obj}/I_{ref} and $\varphi_{obj}/\varphi_{ref}$, respectively. Then, the Stokes parameter is $S_0=I_{obj}$, and the interference pattern (I_{inter}) of such two beams can be deduced as:

$$I_{inter}(r, \phi) = I_{obj}(r, \phi) + I_{ref}(r, \phi) + 2\sqrt{I_{obj}(r, \phi)I_{ref}(r, \phi)} \cos(\varphi_{obj}(r, \phi) - \varphi_{ref}(r, \phi) - \varphi_{del}) \quad (9)$$

Where φ_{del} represents the extra phase delay in reference beam and can be adjusted by the delay line (DL in Fig.2). Since the reference light beam is the 0-order LG mode, the phase distribution of reference light satisfies $\varphi_{ref}(r, \phi) \propto r^2$ in the condition that the optical axis of the reference light beam coincides with the optical axis of detector. For LG mode, the phase factor is proportional to r^2 and $e^{ikr^2/2R}$ determines the radius of the curvature of the wavefront. Thus, the phase term of $\varphi_{obj}(r, \phi) - \varphi_{ref}(r, \phi)$ is equivalent to the phase of a light beam with the same features in terms of Stokes parameters, the topological charge and the direction of propagation, as the objective light beam only except for the curvature radius of the wavefront. And the

topological charge of objective light beam can be calculated after substituting the $\varphi_{obj}(r, \Phi) - \varphi_{ref}(r, \Phi)$ into Eq. (7) as the φ . In principle, two different but arbitrary values of φ_{del} are needed to extract the phase distribution of $\varphi_{obj}(r, \Phi) - \varphi_{ref}(r, \Phi)$. Here, two values of φ_{del1} and φ_{del2} with the relation of $\varphi_{del2} = \varphi_{del1} + \pi/2$ are adopted to achieve the maximum signal-to-noise ratio of the calculated phase distribution. By recording the interference patterns as I_{inter1} and I_{inter2} with corresponding phase delay of φ_{del1} and φ_{del2} , respectively, the phase distribution can be obtained as:

$$\varphi_{obj}(r, \phi) - \varphi_{ref}(r, \phi) = \arg(I_{inter1}(r, \phi) - I_{obj}(r, \phi) - I_{ref}(r, \phi), I_{inter2}(r, \phi) - I_{obj}(r, \phi) - I_{ref}(r, \phi)) \quad (10)$$

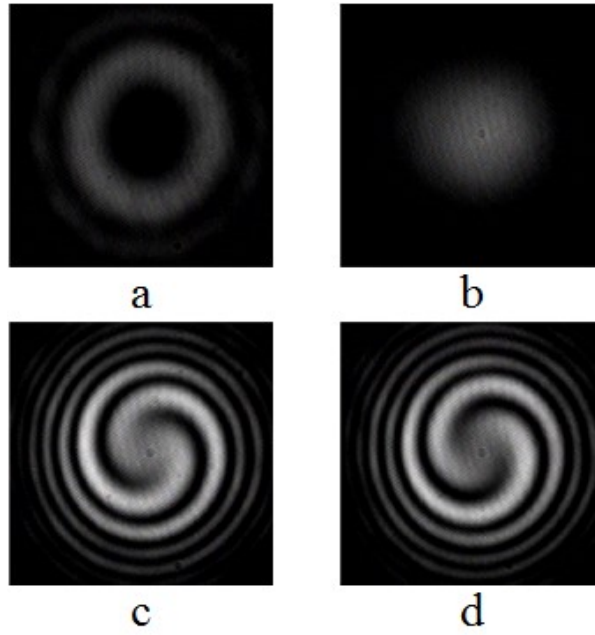


Fig. 3. (a) $I_{obj}(r, \phi)$: the intensity of pre-settled OAM mode beam (objective beam), (b) $I_{ref}(r, \phi)$: the intensity of reference light beam, (c) $I_{inter1}(r, \phi)$ and (d) $I_{inter2}(r, \phi)$: interference intensities of objective beam and reference beam.

As an example, Fig. 3 shows the measured results obtained with the objective beam of -2-order OAM beam. Figure 3(a) and (b) are the intensity patterns of the objective and reference beams ($I_{obj}(r, \Phi)$ and $I_{ref}(r, \Phi)$), while Fig. 3(c) and (d) are the interference patterns of $I_{inter1}(r, \Phi)$ and $I_{inter1}(r, \Phi)$. In both Fig. 3(c) and (d), there are two petals that coincide with the -2-order OAM of the objective beam. Moreover, the interference pattern of Fig. 3(d) rotates half a quarter circumference compared with Fig. 3(c), which is also accordant to additional phase delay of $\pi/2$ in Fig.3 (d).

Results:

Measure the Tilt Angle

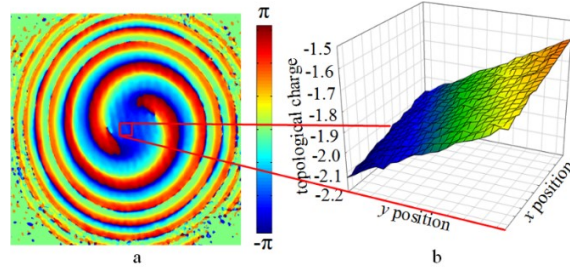


Fig. 4. (a) The phase distribution of the objective beam carried -2-order OAM, and the red box section denotes the boundary of the reference axes adopted to calculate the topological charges. (b) The topological charges calculated with different reference axes (21×21 axes are chosen to reduce the fluctuations) and the x - y coordinate denotes the position of reference axes while the vertical coordinate denotes the corresponding topological charge. As mentioned in Principle section, to obtain the tilt angle between the objective light beam and the optical axis, the topological charge with different reference axes, which are parallel to optical axis, should be calculated. The results are shown in Fig. 4. Figure 4(a) shows the phase distribution of the -2-order OAM objective beam, and the red box section denotes the boundary of the chosen reference axes. Figure 4(b) shows the calculated topological charge with different reference axes.

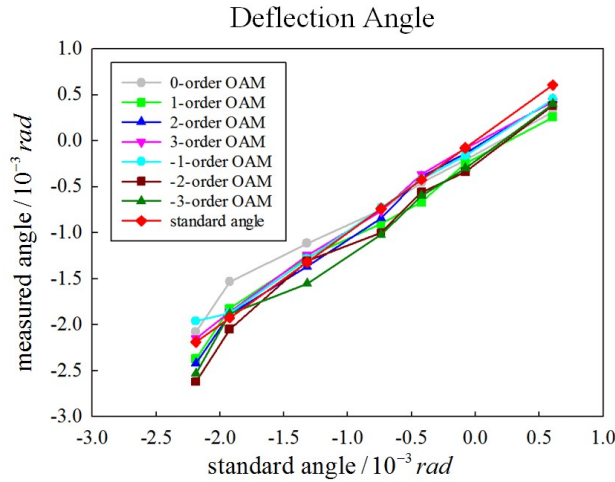


Fig. 5. The measured tilt angle, with OAM beams of -3~3 order. The horizontal coordinate denotes the standard tilt angles obtained by Michelson interference while the standard tilt angle is plotted as a diamond line with slope of 1.

As shown in Fig.4 (b), the calculated topological charge is nearly linearly proportional to the position of reference axis as the prediction in the Principle section. Thus, by calculating the gradient, the tilt angle between the objective beam and the optical axis can be obtained. In our experiments, the light beam carrying OAM with orders of -3~3 are adopted as the objective light beams. Meanwhile, the tilt angle is also measured by Michelson interference and the measured value is denoted as standard angle as reference. The measured tilt angles versus the standard angles are summarized in Fig. 5. For more clarity, the standard tilt angle is plotted as a hollow diamond line with slope of 1 for comparison. From Fig.5, it could be found that the tilt angles measured by our method are well consistent with the standard values and the precision in our system is around $10^{-4}rad$.

Correct the OAM spectrum

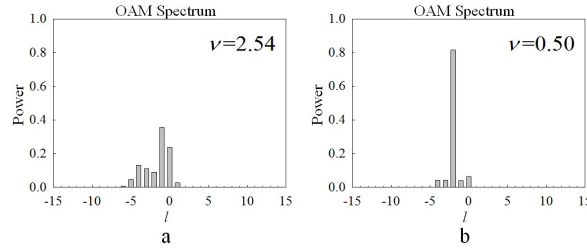


Fig. 6. (a) and (b) shows the results of the measured OAM spectrum, and the corrected OAM spectrum with objective beam of

-2-order OAM and tilt angle of $-3.37 \times 10^{-4}rad$, and the OAM spectrum dispersion factor of $\nu = \frac{\sum C_l l^2}{\sum C_l l} - (\frac{\sum C_l l}{\sum C_l})^2$ is

also presented.

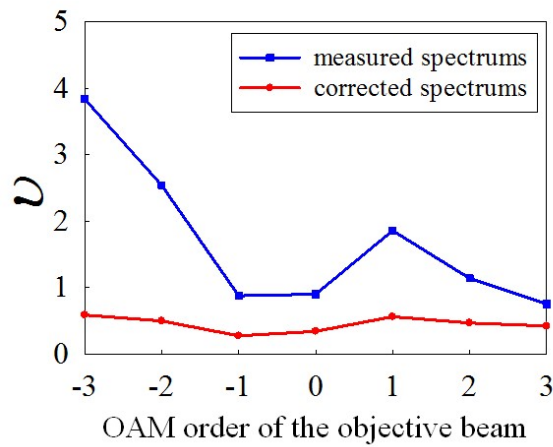


Fig. 7. The dispersion factor of measured OAM spectrums and corrected OAM spectrums. The objective beams are -3~3-order OAM beams.

After measuring the tilt angle, the next step is correcting the OAM spectrum by correcting the measured phase distribution as mentioned above. A typical result is shown in Fig. 6. The pre-settled objective light beam is the -2-order OAM, which is the same as the sample in Fig. 3 and Fig. 4. With the tilt angle of $-3.37 \times 10^{-4} \text{ rad}$, the measured spectrum (Fig. 6(a)) shows multiple lines on OAM spectrum instead of one single peak in the position of -2-order. After correction, as shown in Fig. 6(b), the OAM spectrum is well corrected by our method, although there are some residual components. In order to quantitatively evaluate such correction, the OAM spectrum dispersion factor of $\nu = \sum_l C_l l^2 - (\sum_l C_l l)^2$ is calculated. Obviously, if the dispersion factor is $\nu=0$, it means that there is no degradation. In Fig.6, the value is $\nu=2.54$ for the directly measured OAM spectrum while that is improved to $\nu=0.50$ for the corrected OAM spectrum. Although, the dispersion factor did not achieve the ideal value of $\nu=0$, the improvement is very remarkable. In our experiments, -3~3-order OAM beams has been employed as the objective beam and the full spectrums with and without correction are shown in the supplementary. Here, Fig. 7 shows the summarized result of the dispersion factor ν of measured and corrected OAM spectrums as a comparison. It can be found that the dispersion factor is improved to $\nu=0.3\sim 0.6$ with our correction method.

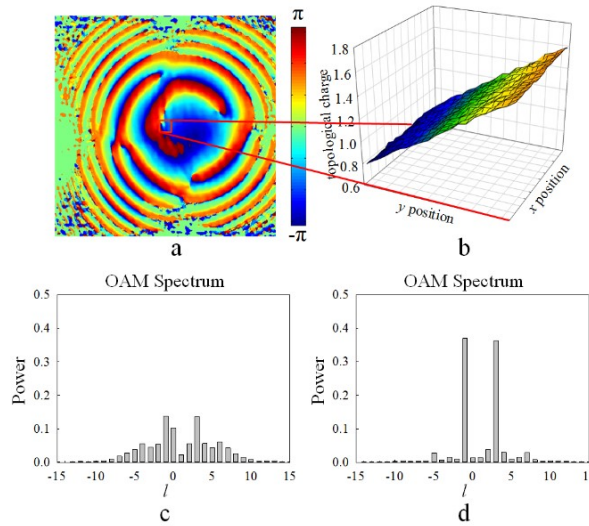


Fig. 8. The experimental results for 3-order and -1-order OAM superposition beam with power ratio of 50:50. (a)

The intensity of objective beam, and the red shadow section denotes boundary of the reference axes used to

calculate the topological charges. (b) The topological charges calculated with different reference axes and the horizontal coordinate denotes the position of reference axes while the vertical coordinate denotes the corresponding topological charge. c) directly measured OAM spectrum. d) corrected OAM spectrum.

In the above section, the objective beam only carries one pure order OAM. Actually, our method can also be applied on the light beams with superposition OAM states. As a concrete example, the superposition of 3-order and -1-order OAM light beam is chosen as the objective beam. The power ratio between 3-order and -1-order component is settled as 50:50 for the objective beam. The intensity of objective beam is shown in Fig. 8(a) while Fig. 8(b) is the total topological charges with different reference axes. From the result of Fig. 8(b), the tilt angle can be obtained as $-6.15 \times 10^{-4} \text{ rad}$. Figure 8(c) and (d) shows the direct measured OAM spectrum and the corrected OAM spectrum, respectively. It could be seen that the OAM spectrum has been well corrected for the light beam carrying superposition of two OAM modes. More results of superposition OAM beams are shown in supplementary.

Discussion:

Till now, our method to deal with optical axis tilt in OAM applications has been demonstrated. The whole procedure could be summarized. First, the field intensity distribution of objective light beam is detected with a CCD camera. Further, by measuring two interference patterns of objective beam and a Gaussian beam, the phase distribution of the objective light field is obtained so that the topological charges of light with different reference axes can be calculated. After that, the tilt angle can be obtained from the slope of topological charge versus the position of reference axis. Once the tilt angle is identified, one option is aligning the optical axis according to it and the other is applying the second-step of our proposed method to correct the OAM spectrum. For some applications, the received light beam or photons would be processed further, *e.g.* optical wireless communication or quantum entanglement, it is inevitable to adjust the optical system since the OAM carried by each photon has truly changed. However, if there is no further manipulation on the received light beam and only origin OAM spectrum is required, there is no necessary to adjust the optical system since our proposed method does not rely on the alignment of optical axis.

Additionally, it should be mentioned that the key point of our method is to obtain the tilt angle from the topological charge diversity with different reference axes. But the result is independent to the method of measuring the topological charge so that one can employ any methods to obtain it, *e.g.* OAM hologram and

optical transformation elements. Here, the reason of measuring the field distribution of light beam in this work is only due to the applicability of any light beam and convenience of implementation. Moreover, the interference method to obtain the phase distribution of objective beam is also replaceable and any other method, *e.g.* computational optical method, can also be adopted.

At last, although the LG modes are chosen as the objective beams in this work, it should be mentioned that there is a similar analysis and relationship between the tilt angle and the topological charge diversity for any light beam and obviously, such relationship would be more complicated. Thus, our proposed method can be extended for any light beams with similar procedure but modified calculation and correction formulae.

In this paper, the OAM topological charges of light beam with different reference axes have been deduced and a two-step method to identify the tilt angle and correct the OAM spectrum of misaligned light beam without iteration is proposed and demonstrated in success. In our experiment, the field intensity and phase distribution of light beam are measured with a CCD camera so that the tilt angle of optical axis is obtained. With employing OAM beams with -3~3-orders as the objective beams, and the precision of measuring tilt angles is about $10^{-4}rad$. After that, the OAM spectrum can be corrected without adjusting the optical axis and for pure OAM state beams, the dispersion factors can be improved from 0.8~3.9 to 0.3~0.6 with our correction algorithm. Moreover, the spectrum correction is also demonstrated with beams of superposed OAM states.

References

1. Allen, L., Beijersbergen, M. W., Spreeuw, R. J. C. & Woerdman, J. P. Orbital angular momentum of light and the transformation of Laguerre-Gaussian laser modes. *Phys. Rev. A* **45**, 8185 (1992).
2. T O'Neil, A. & Padgett, M. J. Three-dimensional optical confinement of micron-sized metal particles and the decoupling of the spin and orbital angular momentum within an optical spanner. *Opt. Commun.* **185**, 139–143 (2000).
3. He, H., Friese, M. E. J., Heckenberg, N. R. & Rubinsztein-Dunlop, H. Direct observation of transfer of angular momentum to absorptive particles from a laser beam with a phase singularity. *Phys. Rev. Lett.* **75**, 826 (1995).
4. Ashkin, A. Forces of a single-beam gradient laser trap on a dielectric sphere in the ray optics regime. *Biophys. J.* **61**, 569 (1992).
5. Simpson, N. B., McGloin, D., Dholakia, K., Allen, L. & Padgett, M. J. Optical tweezers with increased axial trapping efficiency. *J. Mod. Opt.* **45**, 1943–1949 (1998).

6. O'Neil, A. T. & Padgett, M. J. Axial and lateral trapping efficiency of Laguerre–Gaussian modes in inverted optical tweezers. *Opt. Commun.* **193**, 45–50 (2001).
7. Wang, J. *et al.* Terabit free-space data transmission employing orbital angular momentum multiplexing. *Nat. Photonics* **6**, 488–496 (2012).
8. Zhang, D., Feng, X. & Huang, Y. Encoding and decoding of orbital angular momentum for wireless optical interconnects on chip. *Opt. Express* **20**, 26986–26995 (2012).
9. Vaziri, A. *Entanglement of the orbital angular momentum states of photons*. (na, 2001).
10. Vaziri, A., Weihs, G. & Zeilinger, A. Experimental Two-Photon, Three-Dimensional Entanglement for Quantum Communication. *Phys. Rev. Lett.* **89**, (2002).
11. Lavery, M. P., Berkhout, G. C., Courtial, J. & Padgett, M. J. Measurement of the light orbital angular momentum spectrum using an optical geometric transformation. *J. Opt.* **13**, 064006 (2011).
12. Vasnetsov, M. V., Pas'ko, V. A. & Soskin, M. S. Analysis of orbital angular momentum of a misaligned optical beam. *New J. Phys.* **7**, 46–46 (2005).
13. Zambrini, R. & Barnett, S. M. Quasi-Intrinsic Angular Momentum and the Measurement of Its Spectrum. *Phys. Rev. Lett.* **96**, (2006).
14. Liu, Y.-D., Gao, C., Qi, X. & Weber, H. Orbital angular momentum (OAM) spectrum correction in free space optical communication. *Opt. Express* **16**, 7091–7101 (2008).
15. Lin, J., Yuan, X.-C., Chen, M. & Dainty, J. C. Application of orbital angular momentum to simultaneous determination of tilt and lateral displacement of a misaligned laser beam. *JOSA A* **27**, 2337–2343 (2010).
16. Gibson II, G. *et al.* Increasing the data density of free-space optical communications using orbital angular momentum. in (eds. Ricklin, J. C. & Voelz, D. G.) 367 (2004). doi:10.1117/12.557176
17. Uribe-Patarroyo, N., Fraine, A., Simon, D. S., Minaeva, O. & Sergienko, A. V. Object identification using correlated orbital angular momentum states. *Phys. Rev. Lett.* **110**, 043601 (2013).
18. Zhang, D., Feng, X., Cui, K., Liu, F. & Huang, Y. Identifying Orbital Angular Momentum of Vectorial Vortices with Pancharatnam Phase and Stokes Parameters. *Sci. Rep.* **5**, 11982 (2015).
19. Molina-Terriza, G., Torres, J. P. & Torner, L. Management of the Angular Momentum of Light: Preparation of Photons in Multidimensional Vector States of Angular Momentum. *Phys. Rev. Lett.* **88**, (2001).

Acknowledgments

This work was supported by the National Natural Science Foundation of China (Grant No. 61675112 and 61321004) and the National Basic Research Program of China (No. 2013CBA01704 and No. 2013CB328704).

Author Contributions

P.Z., S.L. and X.F. developed the theory. P.Z. and S.L. ran the numerical simulations. P.Z., S.L. and Y.W. did the experiments. P.Z. and X.F. wrote the paper. K.C., F.L. and W.Z. provided useful discussions. Y.H. revised the manuscript. All authors read and approved the manuscript.

Supplementary Information

Identifying the tilt angle and correcting the orbital angular momentum spectrum dispersion of misaligned light beam

Peng Zhao, Shikang Li, Yu Wang, Xue Feng*, Kaiyu Cui, Fang Liu, Wei Zhang, and Yidong Huang

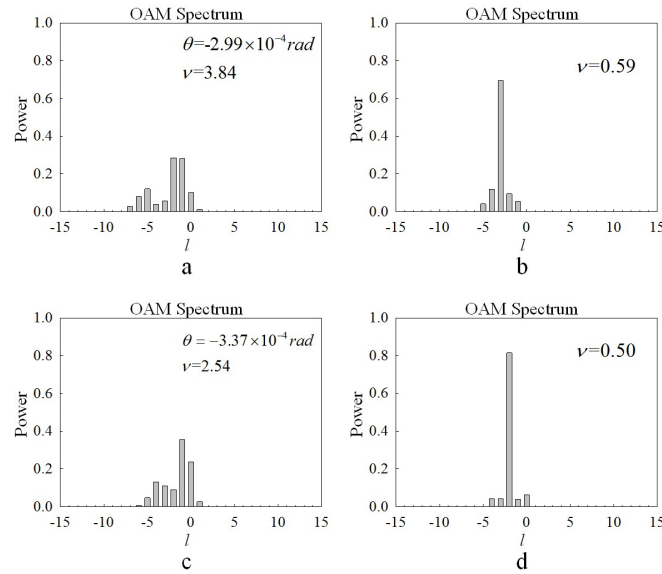
Department of Electronic Engineering, Tsinghua National Laboratory for Information Science and Technology, Tsinghua University, Beijing, China

x-feng@tsinghua.edu.cn

To demonstrate the generality of our method, pure OAM state beams of -3~3-order and several superposition OAM beams are adopted as the objective light beam, respectively. Here we show the results of OAM spectrum correction.

Pure state OAM beams:

Figure 1 shows the measured OAM spectrums and the corrected OAM spectrums. (a), (c), (e), (g), (i), (k) and (m) shows the measured OAM spectrums of -3~3-order OAM beams, respectively, while (b), (d), (f), (h), (j), (l) and (n) shows the corresponding corrected OAM spectrums. In figures of measured OAM spectrums, the tilt angle θ and dispersion factor ν are labeled while in figures of corrected OAM spectrums, only the dispersion factor ν are labeled.



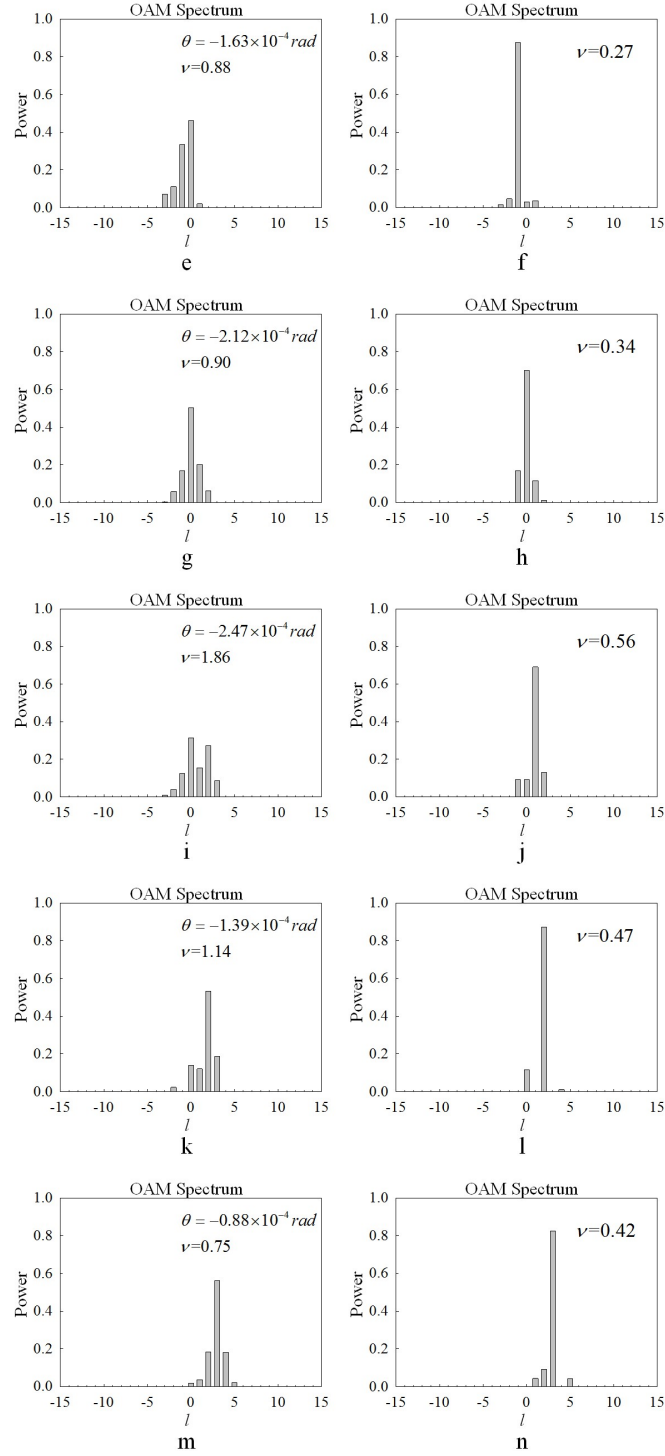


Fig. 1. The measured OAM spectra and the corrected OAM spectra. (a), (c), (e), (g), (i), (k) and (m) shows the measured OAM spectra of -3~3-order OAM beams, respectively, while (b), (d), (f), (h), (j), (l) and (n) shows the corresponding corrected OAM spectra.

Superposition OAM beams:

Figure 2(a) shows the measured OAM spectrum of 3-order and 0-order OAM superposition beam with tilt angle of $-4.60 \times 10^{-4} \text{ rad}$, while (c) shows the measured OAM spectrum of 3-order and -3-order OAM superposition

beam with tilt angle of $-4.15 \times 10^{-4} \text{ rad}$. Fig. 2(b) and (d) show the corrected OAM spectrum corresponding to (a) and (c), respectively.

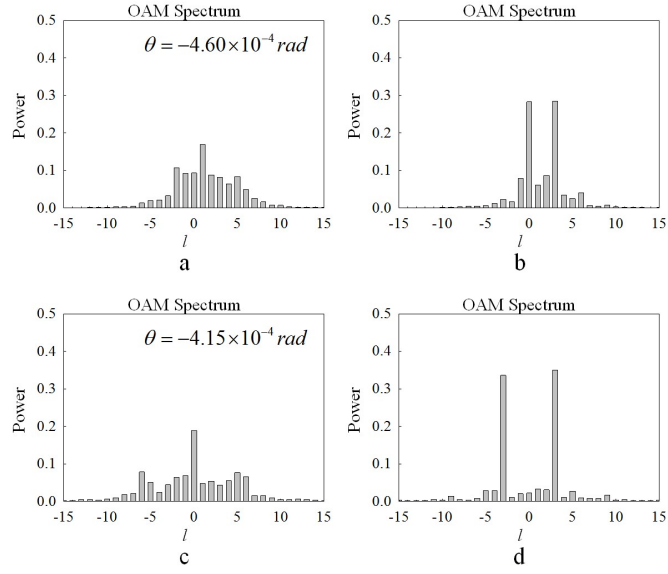


Fig. 2. (a) shows the measured OAM spectrum of 3-order and 0-order OAM superposition beam with tilt angle of $-4.60 \times 10^{-4} \text{ rad}$, while (c) shows the measured OAM spectrum of 3-order and -3-order OAM superposition beam with tilt angle of $-4.15 \times 10^{-4} \text{ rad}$. (b) and (d) show the corrected OAM spectrum corresponding to (a) and (c), respectively.